Role of the C-Terminal Extrinsic Region of the α Polypeptide of the Light-Harvesting 2 Complex of *Rhodobacter sphaeroides*: A Domain Swap Study†

John D. Olsen,*,‡,§ Bruno Robert,|| C. Alistair Siebert,§ Per A. Bullough,§ and C. Neil Hunter‡,§

Robert Hill Institute for Photosynthesis, Krebs Institute for Biomolecular Research, and Department of Molecular Biology and Biotechnology, University of Sheffield, Western Bank, Sheffield S10 2TN, United Kingdom, and Section de Biophysique des Functions Membranaires, DBJC/CEA and URA CNRS 2096, CEA Saclay, 91191 Gif sur Yvette Cedex, France

Received August 7, 2003; Revised Manuscript Received November 5, 2003

ABSTRACT: The LH1 and LH2 complexes of *Rhodobacter sphaeroides* form ring structures of 16 and 9 protomers, respectively, comprising α and *β* polypeptides, bacteriochlorophylls (Bchl), and carotenoids. Using the LH2 complex as a starting point, two chimeric LH complexes were constructed incorporating the αC-terminal domain of either the *Rb. sphaeroides* LH1 complex or the *Rhodospirillum molischianum* LH2 complex. The LH1 domain swap produced a new red-shifted component that comprised ∼30% of the total absorbance. In the LH1α C-terminal mutant this new red-shifted species acts as the terminal emitter, with the new emission maximum located 10 nm further to the red than for the WT. Raman spectroscopy indicates that a fraction of the B850 Bchls is involved in relatively weak H-bonds, possibly involving the αTrp_{+11} residue within the new αC-terminus, consistent with a more LH1-like character for one of the Bchls. The CD data indicate that the domain swaps have perturbed the native arrangement of the B850 Bchls, including the site energy difference between the α- and *β*-bound Bchls. Thus, the normal energetic structure of the ring system has been disrupted, with one component blue shifted due to the presumed loss of an H-bond donor and the other red shifted by the influence of the new αC-terminal domain. The dichotomous response of the mutants to the carotenoids incorporated, spheroidenone or neurosporene, strongly suggests that the C-terminal region of the α polypeptide is involved in binding a carotenoid. The projection map of the LH1α C-terminal mutant complex was determined in negative stain at 25 Å resolution, and it shows a diameter of 53 Å, compared to 50 Å for the WT. Hence these new spectral properties have not been accompanied by an alteration in ring size.

The light-harvesting complexes of purple bacteria form circular arrays of bacteriochlorophylls capable of collecting and then transferring light energy with high efficiency to the reaction centers (RC).[1] There are essentially two types of light-harvesting complex in purple bacteria, LH1 that associates closely with the RC and LH2, which forms a large peripheral antenna. Structural studies, conducted using both 3D X-ray crystallography and 2D cryoelectron microscopy, have highlighted the interesting diversity of ring sizes represented by these complexes. The LH2 complexes can be subdivided into two families: the nonameric, which includes *Rhodopseudomonas acidophila* (*1*), *Rhodovulum sulfidophilum* (*2*), *Rhodobacter sphaeroides* (*3*), and *Rhodocyclus gelatinosus* (*4*), and the octameric, of which there is only one representative to date, *Rhodospirillum molischianum* (*5*). In LH1 only one ring size has been structurally determined, the 16-membered, found in *Rhodospirillum rubrum* (*6*, *7*) and *Blastochloris viridis* (*8*). The LH1 situation is complicated by the presence of the PufX polypeptide in some bacterial LH1 complexes so that they are likely to form an incomplete ring or an arc with fewer than 16 α*β* pairs present (*9*−*11*, *12*). These variations in the LH aggregation state are relevant to their energy transfer function as the overlapping Bchls form a strongly coupled pigment system which in the larger ring sizes produce a greater red shift of the absorption maximum (*11*, *13*). Thus the absorbance maximum of the Q_y band is typically at 850 nm for LH2 complexes and 875−880 nm for LH1 complexes. In terms of antenna function this generates an energy gradient from the higher energy B850 Bchls in the peripheral antenna LH2 to the lower energy B880 Bchls of the LH1 complex that connects to the RC. An additional functional consequence of the larger LH1 structure is that it can accommodate the RC (*3*, *8*).

Close examination of the polypeptide sequences of the LH1 and LH2 complexes reveals many local differences between them (*14*), some of which have been shown by FT Raman spectroscopy to influence the spectral properties of

† This work was supported by a grant from the Biotechnology and Biological Sciences Research Council (BBSRC), U.K. The Krebs Institute for Biomolecular Research is a designated Biomolecular Sciences Centre of the BBSRC. The Krebs Institute Structural Studies Group is a member of the BBSRC North of England Structural Biology Centre.

* To whom correspondence should be addressed at the Department of Molecular Biology and Biotechnology, University of Sheffield. Tel: +44 (0)114 2224240. Fax: +44 (0)114 2222711. E-mail: j.olsen@shef.ac.uk.

‡ Robert Hill Institute for Photosynthesis.

§ Krebs Institute for Biomolecular Research.

|| Section de Biophysique des Functions Membranaires.

[1] Abbreviations: WT, wild type; Bchl, bacteriochlorophyll; LH, light harvesting; RC, reaction center; ICM, intracytoplasmic membrane; DOPC, 1,2-dioleoyl-*sn*-glycero-3-phosphocholine; *β*-OG, *n*-octyl *β*-D-glucopyranoside; ZCP, zero crossing point; LMP, low melting point.

10.1021/bi035411h CCC: $25.00
Published on Web 12/03/2003

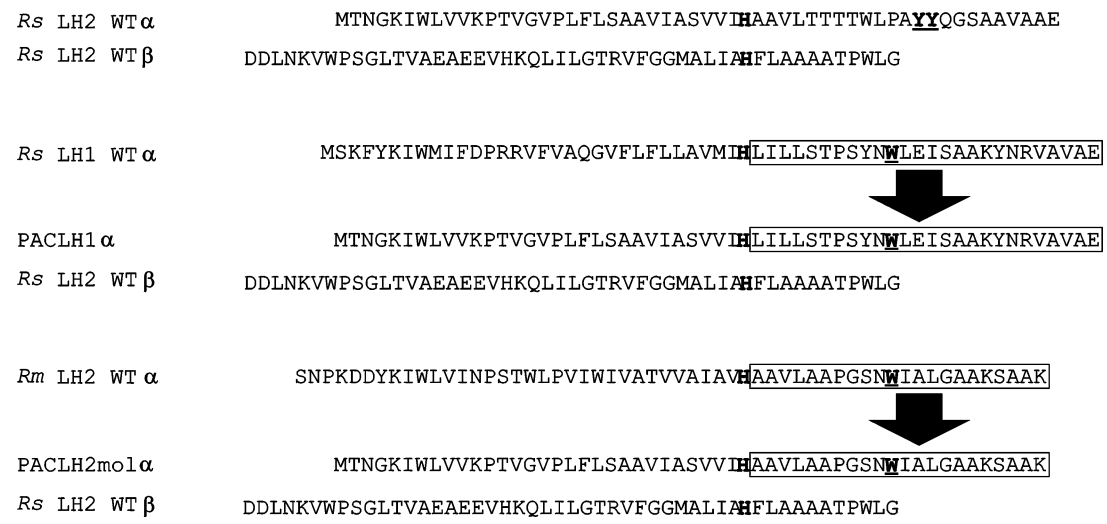

FIGURE 1: Sequence alignment showing the WT *Rb. sphaeroides* (*Rs*) sequences of PucA and PucB together with the sequences of *R. molischianum* (*Rm*) PucA, *Rb. sphaeroides* LH1 PufA, and the chimeric mutants PACLH1 and PACLH2mol. The central conserved His residue is denoted by the bold type, and the residues that form H-bonds to the C2 acetyl carbonyl groups of the Bchls are denoted by the bold underlined letters. The box denotes the region swapped to form PACLH1 and PACLH2mol.

the complex (*15*−*19*, *20*). FT Raman results have revealed the H-bond network in the LH1 of *Rb. sphaeroides* and have demonstrated that it is significantly different from the H-bond network present in the LH2 of *Rb. sphaeroides* (*15*, *17*, *18*, *21*). It is notable that the octameric LH2 of *R. molischianum* has a similar H-bond network to that of *Rb. sphaeroides* LH1 and shares many protein motifs in the αC-terminal region (*22*). Loach and co-workers have shown that an LH1-type complex could be assembled in vitro from highly truncated α and *β* polypeptides (*23*−*26*). While these studies have defined a "minimum core" of the protein, not much is yet known about the functions of the peripheral N- and C-terminal extensions. With the advent of structures to atomic resolution of the LH2 complexes and models of LH1 constructed using the LH2 of *R. molischianum* as a partial template (*27*, *28*), there is increasing interest in assigning functions to the three domains of LH polypeptides. A domain swap approach, in which we "exchange" each domain for equivalents in other LH antennae, should impart information upon the role of these regions in tuning the intra- and intercomplex interactions of the LH2 antenna, as well as its electronic properties. It is noteworthy that multimeric membrane proteins are not uncommon, e.g., ATPase, chaperonins, mechanosensitive channels, and small multidrug resistance proteins, but there is a dearth of information about how they assemble. LH complexes, as multimeric membrane proteins for which two structures are known, offer the possibility of learning the rules by which parallel transmembrane helices associate together in a defined stoichiometry. In that sense, genetic manipulation of the LH2 complex of *Rb. sphaeroides* could yield crucial information on the assembly of multimeric membrane proteins in general.

In this work we have altered the C-terminal sequence of the LH2 α polypeptide of *Rb. sphaeroides* to the equivalent sequence of either the *Rb. sphaeroides* LH1 or the *R. molischianum* LH2, with the eventual objective of attempting to alter the oligomeric structure of the complex from the 9-fold ring of LH2 to a 16-fold LH1 or an 8-fold LH2. In so doing, all of the residues that have been shown to form H-bonds to the B850 Bchls have been changed. Our data reveal that the chimeric complex resulting from the swap with the LH1 C-terminus does have a red-shifted spectral species not seen in the WT LH2 and have shed light on the location of one of the bound carotenoid molecules in the complex. However, the 2D structural data show that the ring size is not significantly different from that of WT LH2. Thus our domain swapping approach has enabled us to begin the construction of new antennae, and it also lays the foundations for determining the other factors responsible for the ring size of LH complexes.

MATERIALS AND METHODS

Strains and Plasmids. Rb. sphaeroides DD13 (*29*), *Rb. sphaeroides* DD13/DG2 (*29*), *Escherichia coli* S17-1 (*30*), pUCHS27:-pUC19, which has had the polylinker *Hin*dIII site blunted out, containing the *puc*BA genes as a *Kpn*I−*Bam*HI fragment (this work), pRKCBC4WT:-pRKCBC1 (*29*) with an engineered *Hin*dIII site between *puc*B and *puc*A and an engineered *Nru*I site just downstream of the *puc*A stop codon (this work), pPACLH1:-pRKCBC4 with a modified *puc*A encoding the C-terminal region of the *puf*A gene of *Rb. sphaeroides* (this work), and pPACLH2mol:-pRKCBC4 with a modified *puc*A encoding the C-terminal region of the *puc*A gene of *R. molischianum* (this work) have been employed.

The *puc*A gene was altered by PCR mutagenesis utilizing a primer that bound to the 3′ end of the *puc*B gene and a reverse primer that "rewrote" the *puc*A gene from the CAC codon of the conserved His residue. For the LH1 swap mutant the new C-terminal sequence was identical to the corresponding 3′ region of the LH1 *puf*A gene, but for the LH2 swap mutant the *R. molischianum* C-terminal protein sequence was encoded using the preferred codons for *Rb. sphaeroides*. The primary sequences of the chimeric LH complexes are shown in Figure 1 with the WT LH2 as a reference.

The PCR was conducted using the ABgene Reddy-Load PCR mix with 100 pmol of forward and reverse primers. The resultant DNA was purified on a LMP gel (Gibco BRL), digested with *Hin*dIII and *Nru*I, and purified on a LMP gel prior to ligation into *Hin*dIII−*Nru*I cut vector pUCHS27. The DNA was checked for the mutant *puc*A gene by

sequencing (ABI "BigDye"). The *puc*BA genes were excised from pUCHS27 as a *Kpn*I−*Bam*HI fragment, gel purified, and ligated into *Kpn*I−*Bam*HI-digested pRKCBC4 to generate the mutant plasmids pRKCBC4PACLH1 and pRKCBC4PACLH2mol, referred to hereafter as pPACLH1 and pPACLH2mol. The modified plasmids were used to transform the conjugation-competent strain *E. coli* S17-1 (*30*). Conjugation was carried out according to the method described in Olsen et al. (*15*). Colonies were examined for the presence of the chimeric LH2 complex using a Guided Wave 260 fiber-optic spectrophotometer and a home-built plate holder. Representative colonies were then grown semiaerobically in liquid culture, and intracytoplasmic membranes (ICM) were isolated as previously described (*15*), except that in this work we used the lower growth temperature of 30 °C and then concentrated the membranes by centrifugation at 186000*g* for 4.5 h after diluting the sucrose present to less than 5% prior to LH purification.

Spectroscopy. Absorbance spectroscopy of the ICMs at room temperature was conducted using a Beckman DU640 spectrophotometer and at 80 K using an Oxford Instruments cryostat and Guided Wave 260 spectrophotometer fitted with a variable path length cell holder.

Fluorescence excitation and fluorescence emission spectra at room temperature were measured with a Jobin Yvon Fluoromax using a 1 cm path length cuvette. For the 80 K measurements the 1 cm cell holder was replaced with a custom mount for the Oxford Instruments cryostat. For the emission fluorescence readings the sample was excited with 590 nm light.

Circular dichroism spectra were recorded on a Jasco J810 spectropolarimeter at room temperature with a resolution of 0.5 nm using a 5 mm path length quartz cell. The sample OD at λ_{max} was adjusted to be ~1 in order to obtain a good signal. Each spectrum is the result of at least three spectra averaged. All spectra were measured with a slit width of 160 μm except those for the WT LH1 complexes, which were measured with a slit width of 300 μm in order to improve the signal to noise ratio.

Fourier transform Raman (FT Raman) spectroscopy in preresonance conditions with the Bchl Q_y transition was performed at 293 K temperature using the 1064 nm excitation from a continuous Nd:YAG laser and a Fourier transform infrared (FTIR) spectrophotometer (Bruker IFS66) equipped with a Raman module (Bruker FRA106) as described in ref *31*.

Deconvolution of Spectra. The spectra were analyzed using the Datamax suite of programs within the Grams/32 package version 4.11 (Galactic Industries Corp.). The following parameters were used in the curve fit: autofind function; maximum number of peaks, 2; sensitivity, medium; fwhh, 15; peak function, Gaussian; baseline function, linear. Initially, these parameters were adjusted manually, and after this coarse adjustment the iteration function of the software was used to minimize the residual. The fit statistics are presented in Table 1 in the Supporting Information, together with figures showing the original absorbance spectra, the Gaussian components, and the residuals for mutant DD13(pPACLH1) and for the WT.

2D Crystallization. Approximately 500 absorbance units of the concentrated ICM sample was solubilized with 1.5 mL of 20% β-OG with gentle stirring at 10 °C and then loaded onto a preequilibrated 15 mL DEAE column. The column was washed for 1 h, at a flow rate of 1 mL/min, with 30 mM NaCl, 10 mM Tris, pH 7.5, and 1% β-OG and then eluted with a 30−400 mM NaCl salt gradient over 60 min, at 1 mL/min. The best fractions were determined by the ratio of the absorbance at ~850 nm vs 280 nm, and these were repurified by loading onto a second DEAE column and rewashing with 30 mM NaCl, 10 mM Tris, pH 7.5, and 1% β-OG for 1 h at a flow rate of 1 mL/min. The elution profile was modified to 30−150 mM NaCl over 60 min, at 1 mL/min, and the best fractions were determined as before. The fraction with the highest ratio was used for 2D crystallization trials using the lipid DOPC; the 2D crystallization and all subsequent electron microscopy and image processing were conducted according to the methods of Walz et al. (*3*).

RESULTS

Absorbance and Fluorescence Spectra. In our mutants, some 40% of the WT sequence has been altered (Figure 1), but nevertheless the chimeric LH2 complexes were assembled in both the DD13 and DD13/DG2 deletion strains. The use of the DD13 and DD13/DG2, *puf* and *puc* double deletion strains allowed us to examine the chimeric complexes even when the levels present in the membrane were low, as there were no other LH complexes present to mask them. The additional flexibility of being able to choose whether to incorporate spheroidenone (DD13) or neurosporene (DD13/DG2) as the major carotenoid allowed us to test for any preference of the chimeric complexes and, in the case of neurosporene, to examine the spectroscopic changes of the carotenoid affected by the novel pigment−protein combinations.

The absorbance spectra of the chimeric complexes at 80 K all exhibit a relative loss of intensity of the "B850" Q_y transition in relation to the B800 band, as measured by the areas of the peaks (data not shown). The B850 peak is shifted to the blue, the opposite of what might be expected if the new complex had acquired the characteristics of an LH1 complex. However, a shoulder is clearly present on the red side of the long-wavelength maximum in the DD13(pPACLH1) spectrum which is not present in the WT control. Thus, domain swapping with the LH1α C-terminal sequence has produced a striking increase in oscillator strength in the red part of the Q_y transition. This qualitative conclusion is the main one to be drawn from these spectra, and in view of the close interactions between B850 Bchls in LH2 (*32*−*34*) this spectral feature cannot be ascribed to a discrete component within the LH ring.

To investigate whether this was likely to be the case for the other domain-swapped mutants, simple visual inspection was inadequate, since any spectral broadening was clearly less pronounced. The absorbance spectra were therefore analyzed by a Gaussian fitting procedure, using the simplest assumption of just two components. The full set of data is displayed in the Supporting Information, together with the deconvoluted spectra and residuals for the two extreme cases of the DD13(pPACLH1) mutant and the WT control. The DD13(pPACLH1) absorbance spectrum was fitted satisfactorily by a major component at 847 nm and a minor one at 872 nm. The same procedure applied to the DD13(pPACLH2mol) spectrum also revealed two possible

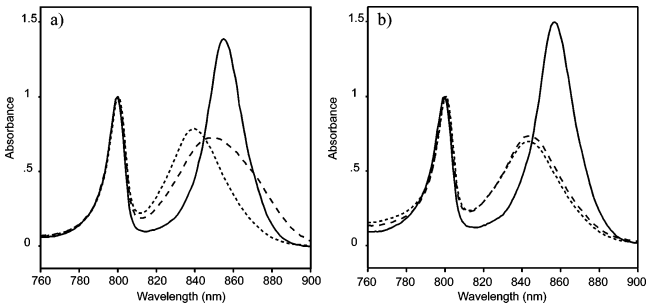

FIGURE 2: Absorbance spectra at 80 K. The spectra have been normalized to the WT B800 band. (a) Complexes expressed in the DD13 (spheroidenone) deletion background. A shoulder can be seen on the red side of the PACLH1 B850 peak. (b) Complexes expressed in the DD13/DG2 (neurosporene) deletion background. Key: solid line, WT; dashed line, PACLH1; dotted line, PACLH2mol.

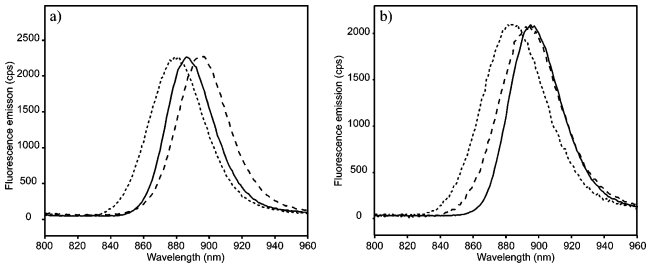

FIGURE 3: (a) Fluorescence emission spectra at 80 K of domain swap complexes in the DD13 (spheroidenone) deletion background. (b) Fluorescence emission spectra at 80 K of domain swap complexes in the DD13/DG2 (neurosporene) deletion background. The amplitudes of the mutant spectra were normalized to the WT emission maximum. Key: solid line, WT;dashed line, PACLH1; dotted line, PACLH2mol.

components, the major one at 840 nm and the minor one at 865 nm. In contrast, the same analysis of the WT spectrum showed no evidence for a pronounced red-shifted component. These effects are more limited when the domain-swapped mutants are expressed in the DD13/DG2 (neurosporene) background.

The fluorescence excitation data at room temperature and 80 K for the domain-swapped mutants in both carotenoid backgrounds (data not shown) support the absorbance data, which indicated the presence of a pool of red-shifted Bchls. The presence of a red-shifted species is most dramatically demonstrated in the fluorescence emission spectrum of DD13(pPACLH1) at 80 K (Figure 3a). The red-shifted species acts as the terminal emitter of the excitation energy, and the emission maximum is located 10 nm further to the red than for the WT. In contrast, the emission maximum for the DD13(pPACLH2mol) complex lies to the blue of the WT maximum. In the neurosporene background (Figure 3b), the red-shifting effect for DD13/DG2(pPACLH1), with respect to the WT, is not seen, although the DD13/DG2(pPACLH1) maximum is 11 nm to the red of the DD13/DG2(pPACLH2mol) maximum. This difference is of the same order as the difference between the emission maxima of the mutants in the DD13 deletion strain.

Absorbance and Fluorescence Spectra at Room Temperature and 80 K: The Carotenoids. In the visible region the spectra of both mutants in the DD13 deletion strain show only a broad, ill-defined absorbance between 400 and 600 nm (data not shown), from which no useful interpretation can be made. In contrast, the mutants in the DD13/DG2 deletion strain have well-defined peaks as expected of neurosporene, which have shifted 2−3 nm to the blue with respect to the WT at room temperature (Table 1), but when measured at 80 K the maxima are nearly coincident with the WT peaks.

Circular Dichroism. The CD spectrum of the WT LH2 is an intense conservative shape with a zero crossing point (ZCP) at 856 nm in the DD13 deletion strain and at 858 nm in the DD13/DG2 deletion strain (Figure 4). In both cases the red shift of the ZCP is 8 nm with respect to the room temperature absorbance spectrum maximum (not shown). In both carotenoid backgrounds the DD13(pPACLH1) mutant has a significantly different spectral shape with a marked decrease in intensity of both the positive and negative lobes, particularly in the latter case. There is a blue shift of the ZCP to 850 nm, which follows the trend of the absorbance maximum. However, it is interesting that the ZCP is now red shifted with respect to the absorbance maximum by ∼11 nm and by ∼12 nm when neurosporene is present in the mutant complex. It is apparent that the B850 Bchls within the DD13(pPACLH1) mutant complex have responded to this domain swap, as already indicated by the absorbance and fluorescence data in Figures 2 and 3; possible reasons for this will be discussed.

The CD spectra for the DD13(pPACLH2mol) mutant resemble those for the LH1 domain-swapped mutant, but the relative position of the ZCP depends on the carotenoid background. In the spheroidenone background the red shift is 9 nm, close to the ZCP red shift for the WT, but when neurosporene is present, the ZCP absorbance red shift is 14 nm. The positions of the ZCP and the room temperature absorbance maxima are summarized in Table 1.

FT Raman Spectroscopy. In view of the differences in H-bonding patterns in the C-terminal regions of LH2 and LH1 complexes revealed by earlier FT Raman studies (*16*−*18*), it was of interest to examine the effects of introducing αC-terminal domain swaps using this technique. The region of the Raman spectrum between 1600 and 1750 cm^{-1} contains bands arising from the stretching modes of the conjugated bond system of the macrocycle. This gives information on the H-bond status of the conjugated acetyl and keto carbonyl groups, as well as on the conformation of the Bchl macrocycles. The five bands at 1628, 1635, 1652, 1679, and 1699 cm^{-1} arising from the acetyl and keto modes have been previously assigned by site-directed mutagenesis of the LH2 complex (*16*). The band at 1635 cm^{-1} arises from the acetyl group of the β-bound Bchl, which forms an H-bond with αTyr_{+13}. The 1628 cm^{-1} band arises from the acetyl of the α-bound Bchl, which interacts with αTyr_{+14}. This mode is degenerate, and there is a second, weak, signal present arising from an H-bond to the acetyl carbonyl of the B800 Bchl. The remaining modes at 1652, 1679, and 1699 cm^{-1} arise from the keto carbonyl stretching modes, the first pair being those to the B850 Bchls and the 1699 cm^{-1} from the B800 Bchl. The DD13/DG2 versions of the mutants did not give a sufficiently good signal to noise ratio to make any useful interpretation of the data; thus only the DD13 versions are reported here.

The modes expected to be affected in the two domain swap mutants are those from the B850 Bchls at 1628 and 1635 cm^{-1} (acetyl carbonyls) and at 1652 and 1679 cm^{-1} (keto carbonyls). In the DD13(pPACLH1) mutant the 1628 cm^{-1}

Table 1: Summary of Spectroscopic Properties of Membrane Samples of the Domain Swap Mutants

		spectroscopic data (nm)					
		DD13 (spheroidenone) background			DD13/DG2 (neurosporene) background		
pigment	property	WT LH2	PACLH1	PACLH2mol	WT LH2	PACLH1	PACLH2mol
Bchls	λ_{max} (RT)[a]	848	839	837	850	836	836
	λ_{max} (80 K)	855	850	840	857	843	843
	CD (ZCP, RT)	856	850	846	858	848	850
Crts	λ_{max} (RT)				432/460/491	−/457/488	−/456/487

[a] RT = room temperature.

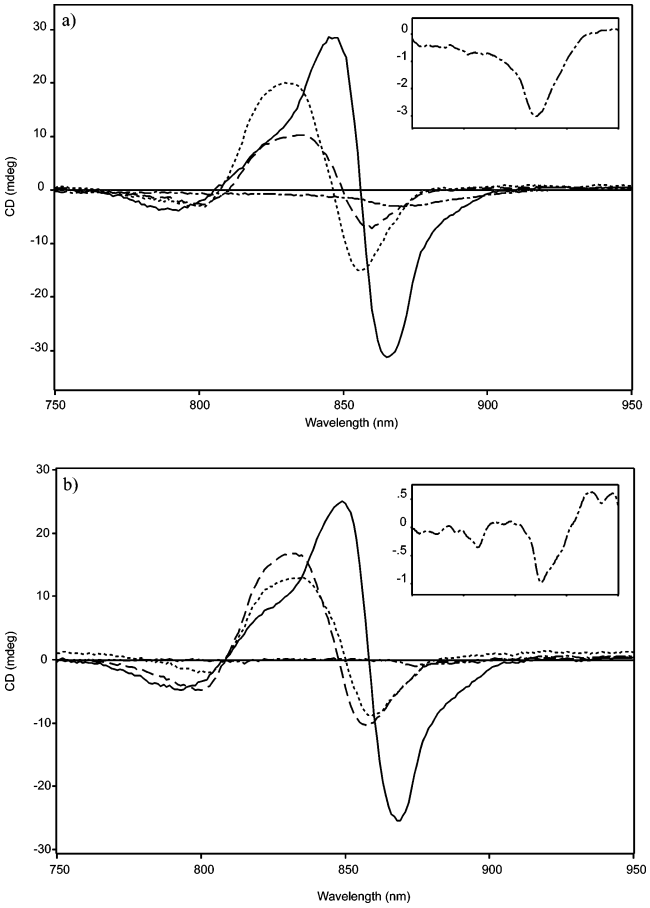

FIGURE 4: Circular dichroism spectra at room temperature. The spectra have been adjusted with respect to their B850 absorbance, and an instrument baseline spectrum has been subtracted. (a) Complexes in the DD13 (spheroidenone) deletion background. (b) Complexes in the DD13/DG2 (neurosporene) deletion background. Key: solid line, WT; dashed line, PACLH1; dotted line, PACLH2mol; dot−dash line, LH1 WT. The insets show the LH1 spectra in order to highlight the very weak CD signals for the LH1 complexes in both carotenoid backgrounds.

band has decreased in intensity, and the 1635 cm^{-1} band has also been affected (Figure 5). These changes are accompanied by the appearance of new signals at approximately 1640 and 1653 cm^{-1}. The band at 1679 cm^{-1} has downshifted to 1673 cm^{-1} and is broader. Finally, the band at 1605 cm^{-1}, arising from the methine bridge stretching mode, has broadened and upshifted to 1608 cm^{-1}.

The FT Raman spectrum of the DD13(pPACLH2mol) mutant also exhibits large changes to the 1628 and 1635 cm^{-1} bands, with upshifts to 1636 and 1648 cm^{-1}, respectively. This large perturbation must involve the near breakage of the H-bonds involving acetyl carbonyls of the B850 Bchls. There is a marked loss of intensity of the 1652 cm^{-1} band;

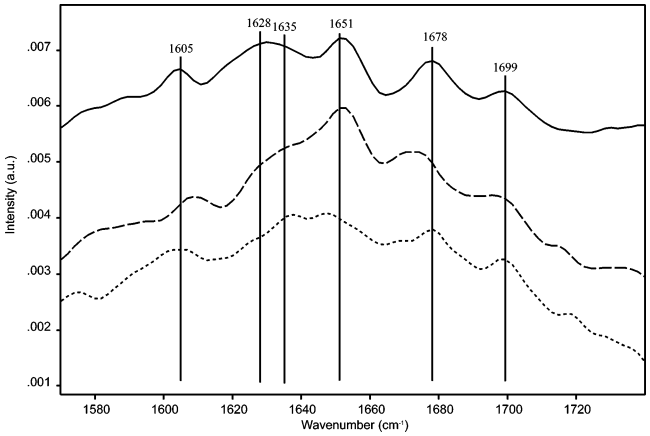

FIGURE 5: FT Raman spectra of the WT and of the DD13-(pPACLH1) and DD13(pPACLH2mol) mutants recorded at room temperature. The spectra have been offset to improve clarity. Key: solid line, WT; dashed line, PACLH1; dotted line, PACLH2mol.

however, the 1678 and 1699 cm^{-1} bands do not appear to be perturbed in this mutant. The band from the methine bridge stretching mode is broadened but is still centered around 1605 cm^{-1}.

2D Crystallization of a Chimeric Light-Harvesting Complex. The C-terminal region of the LH2 α polypeptide was altered to the equivalent sequence for the LH1 complex of *Rb. sphaeroides* and the LH2 of *R. molischianum* with one intention being the alteration of the dimensions of the ring. Earlier C-terminal truncation studies of the LH1 α polypeptide had demonstrated a progressive effect upon aggregation state of the LH1 complex (*9*), thus establishing the importance of this region. Two-dimensional crystallization of purified, solubilized complexes was attempted to test whether the altered spectral properties had been accompanied by altered ring sizes.

The mutant complexes were solubilized in the detergent β-OG and purified by FPLC to ascertain their suitability for 2D crystallization. Of the four mutants (two domain swaps, two carotenoid backgrounds) mutant DD13/DG2(pPACLH1) was sufficiently robust, and 2D crystallization trials were successful. Negatively stained grids of this mutant in the lipid DOPC showed ordered crystals of sufficient quality to produce a projection map at 25 Å resolution (Figure 6). While this map represents the projection of both surfaces of the 2D crystal which is a collapsed vesicle, adjacent LH2 rings alternate in their apparent density, corresponding to "up" and "down" views of the complex as described by Walz et al. (*3*) and also Scheuring et al. (*35*) for WT LH2. The variation in the density of the stain (Figure 6c) arises from slight differences in staining behavior, depending on which side of a particular complex is interacting with the carbon

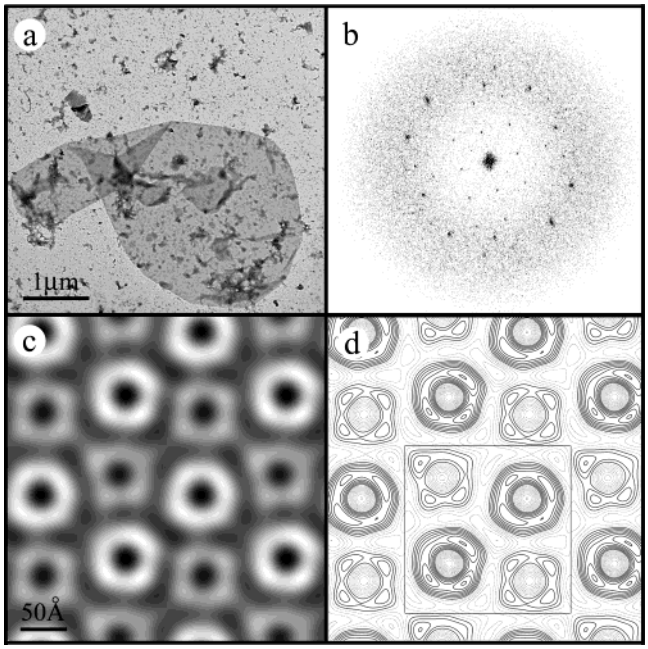

FIGURE 6: (a) Negatively stained 2D crystal of the purified DD31/DG2(pPACLH1) domain swap mutant. (b) A raw Fourier transform. (c, d) Gray scale and contour maps calculated after unbending (*49*) and after correlation averaging (*50*). The scale is the same for both images. The unit cell is as shown in (d); $a \approx b \approx 179$ Å and $\gamma = 90°$. The map resolution is ~25 Å.

support and which side is exposed to the microscope vacuum. However, at this level of resolution the only definitive result that can be derived is the diameter of the ring, which after symmetrization averages as 53 Å. The LH2 WT ring size, also measured from negative stained crystals, is 50 Å (*3*). From these data, and given that the experimental uncertainty is ±10%, we predict that the number of protein subunits present in the mutant is the same as in the WT. These crystals are not of sufficient quality to use in cryoelectron microscopy, but further work is being conducted using DD13(pPACLH1) complexes in the hope that these will produce better quality crystals.

DISCUSSION

Relationship between the C-Terminal Domain of the LH2 α *Polypeptide, H-Bonding, and Spectral Red Shift.* This work reports the first extensive domain exchange exercise on a light-harvesting complex and the low-resolution structural data of one of the resultant mutants. The present study set out to establish if an LH1-type αC-terminus could result in a red shift of some or all of the Bchl absorbance in an LH2 complex and could even change the aggregation state of the complex. Our work has generated two chimeric LH complexes containing a new αC-terminal domain, either from the *Rb. sphaeroides* LH1 complex or from the *R. molischianum* LH2 complex. In the latter case the αC-terminal sequence bears a resemblance to LH1α subunit (*22*). The *R. molischianum* α polypeptide contains elements of both the LH2 and the LH1 sequences but differs from the former in that it lacks one very important motif, $Tyr_{+13}Tyr_{+14}$ (Figure 1). In the basic αβ protomer of LH2 from *Rb. sphaeroides* this motif is responsible for the formation of the two H-bonds to the acetyl carbonyl of the pair of Bchls (*16*). The breakage of one or both of these H-bonds is already known to be accompanied by blue shifts of the λ_{max} of the mutant complexes of 11 and 26 nm, respectively, at 77 K (*36*). Although the normal double H-bonding pattern seen for WT LH2 cannot occur in the two chimeric complexes, the new C-terminal regions could in principle each provide one "new" H-bond from the αTrp_{+11} residue seen in the LH1 complex (*15*) and in the *R. molischianum* complex (*22*), giving a net loss of one H-bond. This would be remarkable, since it would mean that it was possible to use these regions in a modular fashion to build new complexes and even create new H-bonding arrangements, in this case producing mutants with the B800−839 absorbance spectra seen in the single H-bond mutant in Fowler et al. (*16*). We have observed that this is the case, with each domain-swapped mutant exhibiting a blue shift. In this context of weakened or missing H-bonds, therefore, the appearance of the 872 nm red-shifted species in the DD13(pPACLH1) mutant is all the more interesting, suggesting that this domain swap has imparted some LH1 character to the mutant complexes, in terms of red-shifting part of the absorbance of the complex.

Raman spectroscopy was used in order to investigate the possibility that, of the two Bchl C2 acetyl groups present in each αβ protomer in these mutants, one can interact with the αTrp_{+11} residue of the newly introduced αC-terminus. The upshift seen in the Raman spectra to ~1650 cm^{-1} for the DD13(pPACLH1) mutant indicates that most of the acetyl carbonyl oxygens of the B850 Bchls are free from interactions; a similar upshift was seen in the HF(L168) mutant which abolished a C2 acetyl carbonyl H-bond (*37*). However, some of these groups are involved in relatively weak H-bonds, most likely to the new αTrp_{+11} residue, judging by the upshift in frequency from 1635 to 1640 cm^{-1}. It is interesting to note the reverse situation in an LH1 mutant (*15*), in which the replacement of αTrp_{+11} by Tyr resulted in the opposite effect, that is, a downshift from 1640 to 1630 cm^{-1}, because the H-bond was strengthened. We suggest that the new mode at 1640 cm^{-1} found in the DD13(pPACLH1) mutant is analogous to the mode at 1640 cm^{-1} assigned to an H-bond from αTrp_{+11} in the WT LH1 complex (*15*). Another effect of the LH1α domain swap was a broadening and small downshifting of the 1679 cm^{-1} band, indicating an effect on the H-bonded keto carbonyl group. This is consistent with a looser B850 binding pocket, manifested as a range of distances between one of the C9 keto carbonyl groups and the nearby His ligand. Some of these distances are possibly shorter than in the WT leading to a stronger H-bond, a trend continued with the native LH1 complex, which exhibits a mode even further downshifted to 1660 cm^{-1}. An unexpected alteration is the upshifting and broadening of the methine bridge mode from 1605 to 1608 cm^{-1}, which is a clear indication that the shape of one or both Bchl macrocycles has altered. This mode is at ~1605 cm^{-1} in most LH2 complexes whereas for LH1 the value is 1607 cm^{-1} or higher, as in *Rb. sphaeroides* 2.4.1 (*38*). While this is not a definitive indicator, the upshift in this mode for the DD13(pPACLH1) mutant is again consistent with a more LH1-like character for this mutant complex.

Of the H-bonds that could be formed to the B850 Bchl acetyl carbonyls in the DD13(pPACLH2mol) mutant, one is much weaker, and the other is broken. This is seen in Figure 5 as an upshift of the 1628 and 1635 cm^{-1} bands to 1636 and 1648 cm^{-1}, respectively. In the case of the keto carbonyl groups, the marked loss of intensity of the 1652

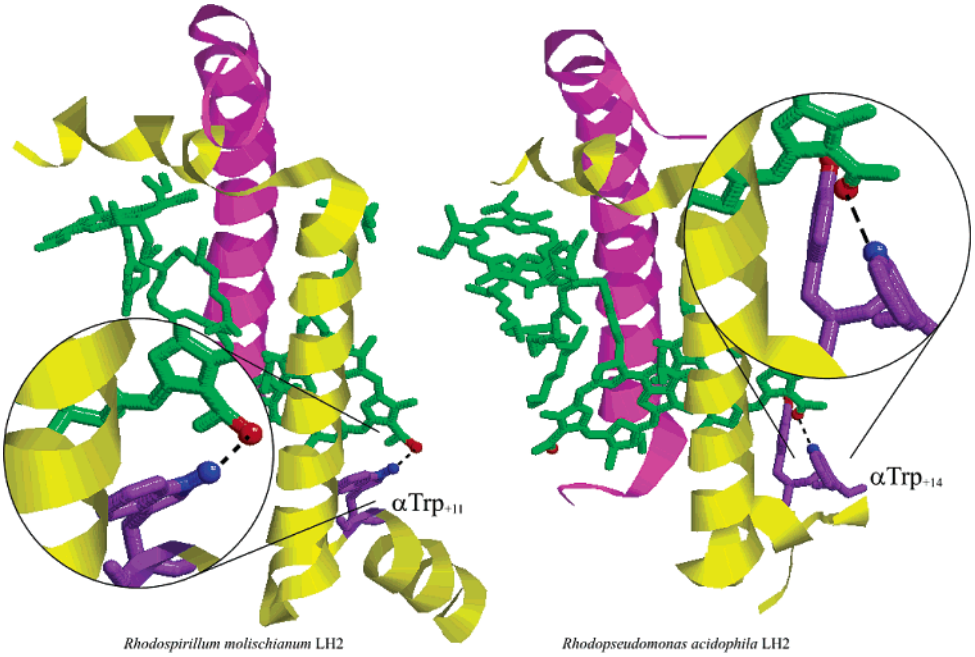

FIGURE 7: Comparison of the C-terminal regions and H-bond arrangements of the LH2 of *R. molischianum* and *Rps. acidophila* 10500. Note the rotation of the C2 acetyl carbonyl group to accommodate the different approach of the Trp residue. The figure was composed using Rasmol (*51*).

cm^{-1} band contrasts with the continued presence of the 1678 cm^{-1} band and suggests that one of these keto carbonyls has undergone a change in its local environment. The methine bridge stretching mode in this mutant is still centered around 1605 cm^{-1} but broadened, which indicates that one or both Bchl macrocycles have undergone a change in shape.

The atomic structure of the αC-terminus of the *R. molischianum* LH2 provides a valuable template of its conformation in its new setting, the *R. sphaeroides* PACLH2mol mutant complex. Furthermore, the similarities of this region with the C-terminal region of the LH1 complex in terms of Raman spectroscopy (*22*) also suggest a mechanism for this region to interact with Bchls in the PACLH1 mutant. The starting point for this domain-swapping study, the *R. sphaeroides* LH2 WT complex, can be approximated with the *R. acidophila* complex, which is structurally similar (*3*). Figure 7 displays $\alpha\beta$ protomers for the *R. molischianum* and *R. acidophila* LH2 complexes to emphasize the difference in arrangements of the C-terminal region, which affect the disposition of the residues and the C2 acetyl carbonyls. While this new C-terminal helix has been accommodated by the PACLH2mol mutant, as evidenced by the presence of an H-bond to one of the C2 acetyl carbonyls, the PACLH1 mutant has only a partial population of H-bonds to one of the C2 acetyl carbonyls. In this context it is possible that the residues closest to the Bchl in the swapped regions of the polypeptides could affect the degrees of freedom of the new C-terminal helix. In the PACLH2mol mutant they are AAVLAAP whereas in the pPACLH1 mutant these residues are LILLSTP. These sequences might explain differences between the domain-swapped mutants in terms of absorbance and Raman data in the 1605 cm^{-1} region. The AAVLAAP residues are for the most part smaller and potentially permit greater flexibility of this region, perhaps allowing the C-terminal helix to adopt a more favorable position, thereby accommodating distortion of the macrocycle observed in the FT Raman results.

Both the DD13(pPACLH1) and PACLH2mol mutants have an increase in oscillator strength in the red end of the red part of the Q_y transition, particularly in the former case. It would appear that the overall energetic disorder of the overlapping Bchls has been increased, with one part of the spectrum blue shifted and the other red shifted by the influence of this new αC-terminal domain. The origin of the red-shifted species is not clear. The upshifting and broadening of the methine bridge mode in the DD13(pPACLH1) mutant indicate the distortion of some of the Bchl macrocycles in the LH2 ring, which could affect the λ_{max} of the Bchl, as predicted (*39*). More recently, it has been postulated that distortion of the B800 Bchl of *Rb. sphaeroides* induces a 150 cm^{-1}, ~10 nm, red shift in its absorbance (*40*). However, this is not the only possibility for inducing a red shift of the mutant complex, and CD was used to provide more insight into the spectral changes provoked by the C-terminal domain swaps.

The CD data for both mutants broadly show a lessening of the amplitude and conservative character of the signal, both seen to a much greater extent in the LH1 complex (see insets in Figure 4). The work of Georgakopoulou et al. (*32*), which examined the CD of a number of types of LH2 antennae as well as modeling the effects of several types of alteration, provides some clues as to the origins of the changes we see for the mutants. While noting that even small alterations can have a large effect on the CD, the following qualitative conclusions can be drawn. The lessening of amplitude is consistent with a small (perhaps less than 5 deg) rotation of either the α- or β-bound Bchl with respect to the plane of the ring. It is also likely that the domain swap has perturbed the site energy difference between the α- or β-bound Bchls, as suggested by the modeling on LH2 CD carried out by Koolhaas et al. (*41*). Both of these effects are consistent with disruption of the native H-bonding arrangement, and since the Raman data indicate that not all of the H-bonding interactions in the ring are affected equally, with

some disrupted and others only weakened, the domain swaps must also have interfered with the symmetry of the system as well. Modeling of this breakage of symmetry, together with 77 K CD spectra of the mutants, would be needed to arrive at a more detailed explanation.

In summary, the introduction of an LH2 αC-terminal domain from the *Rb. sphaeroides* LH1 or *R. molischianum* LH2 complex did not red shift the entire B850 absorbance band in either mutant, but the former mutation did have a marked effect. The DD13(pPACLH1) mutant complex acquired a new red-shifted component that comprised ∼30% of the total absorbance. Thus we appear to have disrupted the normal energetic structure of the ring system: one component has been blue shifted due to the presumed loss of an H-bond donor, and the other has been red shifted by the influence of the new C-terminal domain.

Carotenoid Interactions. The carotenoid region of the absorbance spectra of the mutants expressed in DD13/DG2 at room temperature shows clear shifts of the bands to the blue of the WT positions, the largest shifts being for the DD13/DG2(pPACLH2mol) mutant (Table 1). Similar shifts at room temperature were noticed for purified and membrane-bound LH2 and LH1 complexes containing neuroporene, with the absorbance maxima for LH1 lying up to 6 nm to the blue of those in LH2 (*42*).

One of the most intriguing results in this work is the effect that the bound carotenoid has upon the spectral properties of the two mutant complexes in comparison with the WT and with each other. The absorbance spectra of the two mutants when they incorporate spheroidenone show very different λ_{max} values, DD13(pPACLH1), 850 nm, and DD13(pPACLH2mol), 840 nm, at 80 K, but are identical when they incorporate neurosporene, 843 nm, at 80 K. A similar disparity is observed in the CD data and in the deconvolution data where the complexes incorporating spheroidenone have very different values but those with neurosporene are almost identical. The different carotenoids would appear to be biasing the complexes toward two different polypeptide configurations that in turn dictate the different protein−pigment and pigment−pigment interactions observed. It is difficult to provide a reason why this should be so, as the differences between the two carotenoids are relatively minor, with nine/ten conjugated bonds (neurosporene/spheroidenone) and a methoxy moiety on the latter. The longer conjugated bond system would render spheroidenone more rigid than neurosporene, particularly in the region of the methoxy moiety. We do not have any information as to where this region of the carotenoid is in relation to the other components of the complex in *Rb. sphaeroides*, although the refined structure of LH2 from *Rps. acidophila* 10050 at 2.0 Å (*43*) places the glucoside headgroup of RG2 in a pocket of three α polypeptide residues, αTrp_{+9}, Ala_{+12}, and Tyr_{+13}, and two β residues, βLeu_{+10} and His_{+11}. It is possible that a functionally similar pocket surrounds the methoxy moiety of one spheroidenone molecule in the mutant complexes, and it is this "anchor" that is responsible for the observed spectral differences in the B850 Bchls in the two carotenoid backgrounds. The effect of neurosporene seen in our work is consistent with the recent demonstration of a specific effect of neurosporene in inducing a weakening of the H-bond between αTyr_{+14} and the acetyl carbonyl group of the α-Bchl in the *Rb. sphaeroides* LH2 complex (*44*). In view of the refined LH2 structure (*43*) alterations in carotenoids at the RG2 position could perturb the carotenoid binding site, which contains αTyr_{+13}, a residue already known to form an H-bond to the β-bound Bchl (*1*, *16*). This mechanism would explain the differences in λ_{max} of the B850 Bchls that we observe for WT LH2 complexes in intracytoplasmic membranes of *Rb. sphaeroides* (this work) in the presence of different carotenoids. The fluorescence excitation spectra obtained from our domain swap mutants (data not shown) indicated small differences in the energy transfer between neurosporene and Bchl pigments in the mutants when compared to the WT, the least efficient transfer being in the DD13/DG2(pPACLH2mol) mutant. From this, one might postulate that the carotenoid is not so intimately connected to the Bchls, consistent with this mutant having more flexibility around the B850 binding site, and this suggests that the C-terminal domain of the α polypeptide is involved in binding a carotenoid.

Altered B800:B850 Ratio. The apparent increase in intensity of the B800 absorption band has been observed before in mutants of the LH2 of *Rb. sphaeroides*, for example, in Fowler et al. (*36*), and this has also been demonstrated in the LH3 of *Rps. acidophila* 7050 when grown at low light levels (*45*). The double mutant, $\alpha Tyr_{+13} \rightarrow Phe + \alpha Tyr_{+14} \rightarrow Leu$ (*36*), exhibited much the same absorption spectrum at 77 K as we have observed for the two chimeric mutants in this work at 80 K, where the B800 peak intensity is much greater than the B850 peak. The possibility that some of the B850 pigment molecules are absent is one explanation for this result. However, when considered in the light of the structure of LH2, assuming that the *Rb. sphaeroides* structure is highly homologous to that of *Rps. acidophila*, this seems unlikely as the Bchls of the B850 ring are so well packed that loss of one of every pair would lead to a serious reduction of structural integrity of the complex. A second possibility is that the alterations to the protein structure have changed the electronic structure of the Bchls and some of the oscillator strength has been transferred to a higher energy level. Work by Koolhaas et al. (*34*) on a B800-minus mutant of *Rb. sphaeroides* LH2 allowed the demonstration of an upper exciton band of the B850 Bchls that was estimated to be located at ∼780 nm. Such a transfer of oscillator strength could then lead to an apparent increase in the intensity of the B800 band in these chimeric mutants. This theory is being examined further by the use of double α subunit mutants, which combine the B800-minus genotype and the C-terminal alterations.

Size of the Ring in Domain-Swapped Complexes. The projection map at 25 Å resolution of the DD13/DG2(pPACLH1) mutant complex is sufficient to establish that we have not increased the size of the complex to the 90 Å seen in negative stain images of the LH1 complex from *Rb. sphaeroides* (*3*). The diameter of the mutant LH2 ring is 53 Å, which compares well with the figure of 50 Å for the LH2 WT in negative stain (*3*). More extensive alterations to LH2 will, at some point, trigger an increase in the size of the complex to reach that of LH1.

The LH2 complex appears to be sufficiently robust to withstand major modification of the α polypeptide C-terminus, in this case to that of the LH1 of *Rb. sphaeroides* or the LH2 of *R. molischianum*. Previously, Ranck et al. (*4*) reported the consequences of substantial truncation of the α

polypeptide C-terminal domain of LH2 of *Rubrivivax gelatinosus*. In their work they presented structural data for the WT and for a thermolysin-treated complex, which had up to 18 residues of the extended C-terminus of the α subunit removed. However, this treatment did not significantly alter the spectral properties of the complex, and it was speculated that these extra residues did not reenter the membrane as had been proposed by Brunisholz et al. (*46*). The alteration of large sections of the LH2 protein to either a non-WT sequence (this work) or an artificial sequence (*47*) has relevance to the wider field of study of cofactor binding sites (*48*) as the changes we have made clearly affect the bacteriochlorophyll B850 binding sites and may point to key residues involved in forming the binding site. We may now envisage further ambitious alterations of other domains of LH2 in order to understand the mechanisms governing the aggregation state of both LH1 and LH2 complexes, its preferences for assembly factors, and the relationship between the aggregation state and the red shift of λ_{max} of the Bchls.

CONCLUSIONS

The premise that the C-terminal region of the α subunit of LH2 has an influence upon the ring size of the complex has not been proven by this work but the results indicate that the chimeric mutant DD13(pPACLH1) does have a red-shifted species, and this suggests that this complex has become more like an LH1 complex. However, the presence of the B800 Bchls in the complex is likely to prevent a larger ring forming due to steric constraints, and it would be logical to add the B800-minus mutation (*34*) to DD13(pPACLH1) to remove this potential obstacle. It should be noted that the B800-minus genotype by itself does not lead to a larger ring size (Olsen et al., unpublished data), and the spectroscopic properties it displays are clearly those of an LH2 complex (*34*). Double mutants that incorporate the B800-minus genotype have the potential to form much larger ring sizes, and it will be enlightening to establish the dimensions of these complexes by electron microscopy. Future work will involve the use of chimeric β subunits in combination with the existing α subunit mutants in a program of work that "titrates" further LH1 elements into the complex.

ACKNOWLEDGMENT

We thank Dr. Peiyi Wang for excellent microscopy support.

SUPPORTING INFORMATION AVAILABLE

A figure and a table showing details of the spectral deconvolutions. This material is available free of charge via the Internet at http://pubs.acs.org.

REFERENCES

1. McDermott, G., Prince, S. M., Freer, A. A., Hawthornthwaite-Lawless, A. M., Papiz, M. Z., Cogdell, R. J., and Isaacs, N. W. (1995) *Nature 374*, 517−521.
2. Savage, H., Cyrklaff, M., Montoya, G., Kühlbrandt, W., and Sinning, I. (1996) *Structure 4*, 243−252.
3. Walz, T., Jamieson, S. J., Bowers, C. M., Bullough, P. A., and Hunter, C. N. (1998) *J. Mol. Biol. 282*, 833−845.
4. Ranck, J. L., Ruiz, T., Pehau-Arnaudet, G., Arnoux, B., and Reiss-Husson, F. (2001) *Biochim. Biophys. Acta 1506*, 67−78.
5. Koepke, J., Hu, X. C., Muenke, C., Schulten, K., and Michel, H. (1996) *Structure 4*, 581−597.
6. Karrasch, S., Bullough, P. A., and Ghosh, R. (1995) *EMBO J. 14*, 631−638.
7. Jamieson, S. J., Wang, P., Qian, P., Kirkland, J. Y., Conroy, M. J., Hunter, C. N., and Bullough, P. A. (2002) *EMBO J. 21*, 3927−3935.
8. Scheuring, S., Seguin, J., Marco, S., Levy, D., Robert, B., and Rigaud, J. L. (2003) *Proc. Natl. Acad. Sci. U.S.A. 100*, 1690−1693.
9. McGlynn, P., Westerhuis, W. H., Jones, M. R., and Hunter, C. N. (1996) *J. Biol. Chem. 271*, 3285−3292.
10. Jungas, C., Ranck, J. L., Rigaud, J. L., Joliot, P., and Vermeglio, A. (1999) *EMBO J. 18*, 534−542.
11. Westerhuis, W. H., Sturgis, J. N., Ratcliffe, E. C., Hunter, C. N., and Niederman, R. A. (2002) *Biochemistry 41*, 8698−8707.
12. Cogdell, R. J., Fyfe, P. K., Barrett, S. J., Prince, S. M., Freer, A. A., Isaacs, N. W., McGlynn, P., and Hunter, C. N. (1996) *Photosynth. Res. 48*, 55−63.
13. Westerhuis, W. H. J., Hunter, C. N., van Grondelle, R., and Niederman, R. A. (1999) *J. Phys. Chem. B 103*, 7733−7742.
14. Brunisholz, R. A., and Zuber, H. (1992) *J. Photochem. Photobiol., B 15*, 113−140.
15. Olsen, J. D., Sockalingum, G. D., Robert, B., and Hunter, C. N. (1994) *Proc. Natl. Acad. Sci. U.S.A. 91*, 7124−7128.
16. Fowler, G. J. S., Sockalingum, G. D., Robert, B., and Hunter, C. N. (1994) *Biochem. J. 299*, 695−700.
17. Olsen, J. D., Sturgis, J. N., Westerhuis, W. H., Fowler, G. J. S., Hunter, C. N., and Robert, B. (1997) *Biochemistry 36*, 12625−12632.
18. Sturgis, J. N., Olsen, J. D., Robert, B., and Hunter, C. N. (1997) *Biochemistry 36*, 2772−2778.
19. Gall, A., and Robert, B. (1999) *Biochemistry 38*, 5185−5190.
20. McLuskey, K., Prince, S. M., Cogdell, R. J., and Isaacs, N. W. (2001) *Biochemistry 40*, 8783−8789.
21. Robert, B., and Lutz, M. (1985) *Biochim. Biophys. Acta 807*, 10−23.
22. Germeroth, L., Lottspeich, F., Robert, B., and Michel, H. (1993) *Biochemistry 32*, 5615−5621.
23. Meadows, K. A., Iida, K., Tsuda, K., Recchia, P. A., Heller, B. A., Antonio, B., Nango, M., and Loach, P. A. (1995) *Biochemistry 34*, 1559−1574.
24. Davis, C. M., Parkes-Loach, P. S., Cook, C. K., Meadows, K. A., Bandilla, M., Scheer, H., and Loach, P. A. (1996) *Biochemistry 35*, 3072−3084.
25. Meadows, K. A., Parkes-Loach, P. S., Kehoe, J. W., and Loach, P. A. (1998) *Biochemistry 37*, 3411−3417.
26. Kehoe, J. W., Meadows, K. A., Parkes-Loach, P. S., and Loach, P. A. (1998) *Biochemistry 37*, 3418−3428.
27. Hu, X., and Schulten, K. (1998) *Biophys. J. 75*, 683−694.
28. Conroy, M. J., Westerhuis, W. H., Parkes-Loach, P. S., Loach, P. A., Hunter, C. N., and Williamson, M. P. (2000) *J. Mol. Biol. 298*, 83−94.
29. Jones, M. R., Fowler, G. J. S., Gibson, L. C. D., Grief, G. G., Olsen, J. D., Crielaard, W., and Hunter, C. N. (1992) *Mol. Microbiol. 6*, 1173−1184.
30. Simon, R., Priefer, U., and Pühler, A. (1983) *Bio/Technology 1*, 784−791.
31. Mattioli, T. A., Hoffmann, A., Sockalingum, D. G., Schrader, B., Robert, B., and Lutz, M. (1993) *Spectrochim. Acta, Part A 49*, 785−799.
32. Georgakopoulou, S., Frese, R. N., Johnson, E., Koolhaas, C., Cogdell, R. J., van Grondelle, R., and van der Zwan, G. (2002) *Biophys. J. 82*, 2184−2197.
33. Koolhaas, M. H., van der Zwan, G., van Mourik, F., and van Grondelle, R. (1997) *Biophys. J. 72*, 1828−1841.
34. Koolhaas, M. H., Frese, R. N., Fowler, G. J. S., Bibby, T. S., Georgakopoulou, S., van der Zwan, G., Hunter, C. N., and van Grondelle, R. (1998) *Biochemistry 37*, 4693−4698.
35. Scheuring, S., Reiss-Husson, F., Engel, A., Rigaud, J. L., and Ranck, J. L. (2001) *EMBO J. 20*, 3029−3035.
36. Fowler, G. J. S., Visschers, R. W., Grief, G. G., van Grondelle, R., and Hunter, C. N. (1992) *Nature 355*, 848−850.
37. Mattioli, T. A., Williams, J. C., Allen, J. P., and Robert, B. (1994) *Biochemistry 33*, 1636−1643.
38. Lapouge, K., Naveke, A., Gall, A., Ivancich, A., Seguin, J., Scheer, H., Sturgis, J. N., Mattioli, T. A., and Robert, B. (1999) *Biochemistry 38*, 11115−11121.

39. Barkigia, K. M., Chantranupong, L., Smith, K. M., and Fajer, J. (1988) *J. Am. Chem Soc. 110*, 7566−7567.
40. Gall, A., Fowler, G. J. S., Hunter, C. N., and Robert, B. (1997) *Biochemistry 36*, 16282−16287.
41. Koolhaas, M. H. C., van der Zwan, G., Frese, R. N., and van Grondelle, R. (1997) *J. Phys. Chem. B 101*, 7262−7270.
42. Hunter, C. N., Pennoyer, J. D., Sturgis, J. N., Farrelly, D., and Niederman, R. A. (1988) *Biochemistry 27*, 3459−3467.
43. Papiz, M., Prince, S. M., Howard, T., Cogdell, R. J., and Isaacs, N. W. (2003) *J. Mol. Biol. 326*, 1523−1538.
44. Gall, A., Cogdell, R. J., and Robert, B. (2003) *Biochemistry 42*, 7252−7258.
45. Gardiner, A. T., Cogdell, R. J., and Takaichi, S. (1993) *Photosynth. Res. 38*, 159−167.
46. Brunisholz, R. A., Suter, F., and Zuber, H. (1994) *Eur. J. Biochem. 222*, 667−675.
47. Braun, P., Olsen, J. D., Strohmann, B., Hunter, C. N., and Scheer, H. (2002) *J. Mol. Biol. 318*, 1085−1095.
48. Gibney, B. R., Rabanal, F., Reddy, K. S., and Dutton, P. L. (1998) *Biochemistry 37*, 4635−4643.
49. Henderson, R., Downing, K., Lepault, J., and Zemlin, F. (1986) *Ultramicroscopy 19*, 147−178.
50. Crowther, R. A., Henderson, R., and Smith, J. M. (1996) *J. Struct. Biol. 116*, 9−16.
51. Sayle, R. A., and Milner White, E. J. (1995) *Trends Biochem. Sci. 20*, 374−376.

BI035411H